THE JOURNAL OF BIOLOGICAL CHEMISTRY VOL. 290, NO. 20, pp. 12603–12613, May 15, 2015

Macrophage-T Cell Interactions Mediate Neuropathic Pain through the Glucocorticoid-induced Tumor Necrosis Factor Ligand System*

Received for publication, January 4, 2015, and in revised form, March 13, 2015 Published, JBC Papers in Press, March 18, 2015, DOI 10.1074/jbc.M115.636506

Yuka Kobayashi[‡], Norikazu Kiguchi[‡], Yohji Fukazawa[‡], Fumihiro Saika[‡], Takehiko Maeda[§], and Shiroh Kishioka[‡1]

From the [‡]Department of Pharmacology, Wakayama Medical University, 811-1 Kimiidera, Wakayama 641-0012 and the [§]Department of Pharmacology, Niigata University of Pharmacy and Applied Life Sciences, 265-1 Higashijima, Niigata 956-8603, Japan

Background: Peripheral neuroinflammation is associated with neuropathic pain.
Results: Inhibiting the glucocorticoid-induced tumor neurosis factor receptor ligand (GITRL) system in infiltrating macrophages and T cells in the injured nerve attenuated neuropathic pain.
Conclusion: GITRL expressed by macrophages drives cytokine release and T cell activation, resulting in neuropathic pain via GITR-dependent actions.
Significance: Macrophage-T cell interactions via the GITRL system provides insights into controlling neuropathic pain.

Peripheral neuroinflammation caused by activated immune cells can provoke neuropathic pain. Herein, we investigate the actions of macrophages and T cells through glucocorticoid-induced tumor neurosis factor receptor ligand (GITRL) and its receptor (GITR) in neuropathic pain. After partial sciatic nerve ligation (PSL) in enhanced green fluorescent protein (eGFP) chimeric mice generated by the transplantation of eGFP$^+$ bone marrow cells, eGFP$^+$ macrophages, and T cells markedly migrated to the injured site after PSL. Administration of agents to deplete macrophages (liposome-clodronate and Clophosome-A^{TM}) or T cells (anti-CD4 antibody and FTY720) could suppress PSL-induced thermal hyperalgesia and tactile allodynia. The expression levels of co-stimulatory molecules GITRL and GITR were increased on infiltrating macrophages and T cells, respectively. The perineural injection of a GITRL neutralizing antibody that could inhibit the function of the GITRL-GITR pathway attenuated PSL-induced neuropathic pain. Additionally, the induction of inflammatory cytokines and the accumulation of GITR$^+$ T cells in the injured SCN were abrogated after macrophage depletion by Clophosome-A^{TM}. In conclusion, GITRL expressed on macrophages drives cytokine release and T cell activation, resulting in neuropathic pain via GITR-dependent actions. The GITRL-GITR pathway might represent a novel target for the treatment of neuropathic pain.

Neuronal damage to the central and peripheral nervous systems often leads to neuropathic pain, which is characterized by tactile allodynia, hyperalgesia, and spontaneous pain. The underlying mechanism of neuropathic pain is highly complex and current analgesic drugs, such as nonsteroidal anti-inflammatory drugs and opioid analgesics, are not effective (1, 2). To develop novel therapeutic strategies, an improved understanding of the mechanisms that drive neuropathic pain is required. Growing evidence indicates that several types of immune cells play crucial roles in chronic neuroinflammation associated with neuropathic pain (3–5). Neuronal damage induces the migration of immune cells, such as macrophages, neutrophils, and T-lymphocytes (T cells), and these cells release inflammatory cytokines (*e.g.* interleukin (IL)-1β and tumor necrosis factor (TNF)-α) and chemokines (*e.g.* monocyte chemoattractant protein-1), triggering chronic neuroinflammation (6). We have previously reported that macrophage inflammatory proteins, which are types of chemokines, are released by activated macrophages and neutrophils following peripheral nerve injury and contribute to the development of neuropathic pain (7–9). Because chemokines can stimulate various types of immune cells, we hypothesized that communication among immune cells promotes neuroinflammation through cytokine and chemokine networks and amplifies pain sensitivity under conditions of neuropathic pain.

It is well known that transmembrane immunomodulatory molecules expressed by immune cells can co-stimulate or co-inhibit cell interactions. Glucocorticoid-induced TNF receptor ligand (GITRL)[2] is a membrane-associated protein, which is mainly expressed on membrane surfaces of antigen-presenting cells, such as macrophages and dendritic cells. GITRL acts on its receptor (glucocorticoid-induced TNF receptor, GITR; also known as TNFRSF18) (10, 11). Activation of the GITRL-GITR pathway enhances T cell proliferation and cytokine production via the T cell receptor (12). The expression of GITR is constitutively low in naive T cells, but becomes increased in activated T cells. Notably, GITR is widely expressed in CD4$^+$ T cells and its function varies among T cell subsets (12). Stimulation of

* This work was supported by Grant-in-Aid for Young Scientists Grant B:23791724 from the Japan Society for the Promotion of Science (Tokyo, Japan).
[1] To whom correspondence should be addressed. Tel.: 81-73-441-0629; Fax: 81-73-446-3806; E-mail: kishioka@wakayama-med.ac.jp.

[2] The abbreviations used are: GITRL, glucocorticoid-induced TNF receptor ligand; GITR, glucocorticoid-induced TNF receptor; PSL, partial sciatic nerve ligation; BMT, bone marrow transplantation; Tg, transgenic; eGFP, enhanced green fluorescent protein; SCN, sciatic nerve; PM, peritoneal macrophage; Treg, regulatory T cell.

GITR in $CD4^+$ effector T cells can enhance cytokine production (*e.g.* interferon-γ and IL-2), whereas GITR stimulation in regulatory T (Treg) cells can suppress excessive immune responses. Hence, the GITRL-GITR pathway has been considered to be important for regulating both innate and adaptive immune responses. Inhibition of the GITRL-GITR pathway prevented the development of autoimmune diabetes and carrageenan-induced acute lung inflammation in mice (13, 14). However, no studies have yet reported the involvement of the GITRL-GITR pathway in peripheral neuroinflammation induced by nerve injury. Herein, we focused on the roles of both macrophages and T cells in neuroinflammation and investigated the function of the GITRL-GITR pathway in partial sciatic nerve ligation (PSL)-induced neuropathic pain.

EXPERIMENTAL PROCEDURES

Animals and Surgery—This study complied with the Ethical Guidelines of the International Association for the Study of Pain. All experimental procedures were approved by the Animal Research Committee of Wakayama Medical University (approval no. 567, Wakayama, Japan). Male mice of the Institute of Cancer Research strain that were 4 or 5 weeks old and weighed 18–25 g were purchased from Nihon SLC (Hamamatsu, Japan) and used for all experiments, except for analyses using bone marrow transplantation (BMT). For BMT, male C57BL/6-Tg (CAG-EGFP) C14-Y01-FM131Osb transgenic (Tg) mice carrying an eGFP allele were obtained from the RIKEN Bioresource Center (Tsukuba, Japan). Wild-type (WT; C57BL/6J) mice were purchased from Nihon SLC. All mice were housed under controlled ambient temperature (23–24 °C, 60–70% relative humidity) and light (lights were on from 8:00 a.m. to 8:00 p.m.) conditions at our institutional vivarium, and had *ad libitum* access to water and food. To induce neuropathic pain, mice were subjected to a PSL operation, as described previously (15, 16). Briefly, under sodium pentobarbital (70 mg/kg) anesthesia, ~1/2 of the sciatic nerve (SCN) thickness was tightly ligated with a silk suture (No. 1, Natsume Seisakusho Co., Tokyo, Japan). In the sham control operations, the SCN was first exposed and then closed without ligation.

Drug Administration—Clodronate disodium salt (Merck Millipore, Billerica, MA), Clophosome-A™ (FormuMax Scientific, Palo Alto, CA), FTY720 (Cayman Chemical, Ann Arbor, MI), anti-CD4 antibody (anti-CD4 Ab; CEDARLANE Laboratories, Burlington, Ontario, Canada), and anti-GITR ligand/TNFSF18 antibody (anti-GITRL Ab; R&D Systems, Minneapolis, MN) were used. Clodronate disodium salt was dissolved in sterile phosphate-buffered saline (PBS) and encapsulated by mixing with COATSOME EL-01-C (NOF Co., Tokyo, Japan) at room temperature to prepare liposome-clodronate. Clophosome-A™ is a commercially available liposome-clodronate reagent and was used without dilution. FTY720 was dissolved in PBS containing 20% dimethyl sulfoxide. Liposome-clodronate, Clophosome-A™, anti-CD4 antibody, and FTY720 were systemically injected. Liposome-clodronate (1 mg in 0.2 ml) was intravenously injected twice (1 day before PSL and 4 days after PSL), and Clophosome-A™ (0.1 ml) was intravenously injected once (1 day before PSL). Anti-CD4 Ab (diluted 1:5) with PBS or control IgG (as a control) was intravenously injected twice (12 and 17 days before PSL) according to a standard protocol described by the manufacturer. FTY720 (0.1 mg/kg) or PBS (containing 20% dimethyl sulfoxide) was intraperitoneally injected once per day for 8 days (days 0–7) after PSL. The administration schedule and dose of FTY720 were similar to those of previous reports (17, 18). Clophosome-A™ or anti-GITRL Ab was perineurally injected, as described in our previous report (7). A total of 10 μl of Clophosome-A™ was injected four times early (just after PSL and days 2, 4, and 6 after PSL) or late (days 7, 9, 11, and 13 after PSL) in the disease model. A total of 10 μl of anti-GITRL Ab or control IgG was injected five times at 3-day intervals (just after PSL and on days 3, 6, 9, and 12 after PSL).

Generation of eGFP-chimeric Mice—We generated eGFP-chimeric mice using BMT as described previously (19, 20). After euthanasia by decapitation, femurs isolated from donor eGFP-transgenic mice were centrifuged in microtubes, and the obtained pellet was suspended in sterile PBS. Recipient WT mice received whole body irradiation with 10 gray for 25 min. A total of 2×10^5 BM cells derived from eGFP-transgenic mice were transplanted into recipient mice by tail vein injection. Then, 3 weeks later, the success of BMT was confirmed by phenotyping peripheral leukocytes collected from tail vein blood.

Pain Assessment—PSL-induced thermal hyperalgesia and tactile allodynia were evaluated by the Hargreaves test and the von Frey test, respectively, as described previously (7, 16, 21). In the Hargreaves test, paw withdrawal latency from radiant heat was measured. Withdrawal latencies were measured three times for each hind paw, and the mean latency time was calculated to evaluate thermal hyperalgesia. In the von Frey test, withdrawal responses were measured using two von Frey filaments (0.07 or 0.16 g). The von Frey filament was applied to the middle of the planter surface of the hind paw and withdrawal responses were measured 10 times for each hind paw. The number of withdrawal responses to mechanical stimulation was calculated. The 50% withdrawal threshold was measured using von Frey filaments of 0.04, 0.07, 0.16, 0.4, and 0.6 g. The percent response to five mechanical stimulations with each filament was converted to a probit value, and the 50% value was evaluated on a linear probit curve using GraphPad Prism 3 (GraphPad Software, La Jolla, CA). Behavioral pain assessments were confirmed by several experimenters to avoid bias. In all behavioral tests, mice received both PSL (left hind paw) and sham (right hind paw) treatment regimens. The PSL-operated hind paw was defined as the ipsilateral side, and the sham-operated hind paw was defined as the contralateral side. The both hind paws were tested using the Hargreaves and von Frey tests. Perineurally injected test and control drugs were administered bilaterally (ipsilateral side and contralateral side), and then each pain threshold was assessed.

Immunohistochemistry—SCN sections were prepared as we described previously (7). Sections were incubated with specific primary antibodies against F4/80 (a macrophage marker, 1:200; CEDARLANE), CD4 (a T cell marker, 1:50; BD Bioscience, San Jose, CA), GITRL (1:50; Abcam Inc., Cambridge, UK), or GITR (1:100; R&D Systems) at 4 °C overnight. Antibodies were diluted in reaction buffer (1% bovine serum albumin and 0.025% PBS-Tween (PBS-T)). Sections were washed with 0.1%

PBS-T and incubated with secondary antibodies conjugated to fluorescent markers (Alexa Fluor-488 or Alexa Fluor-594, 1:200; Invitrogen) for 2 h at room temperature, followed by nuclear staining using Hoechst 33342 solution (1:1000; Invitrogen). A coverslip with Perma Fluor (Thermo Fisher Scientific, Waltham, MA) was placed over the sections and immunoreactivity was detected using a confocal laser-scanning microscope (Carl Zeiss, Jena, Germany).

PCR—Mice were euthanized and SCNs, and peritoneal macrophages (PMs) were freshly isolated. The isolated SCN was cut into 10-mm long sections. To collect PMs from naive mice, an incision was made in the peritoneal membrane and 5 ml of ice-cold sterile PBS containing 1% penicillin-streptomycin was slowly injected into the peritoneal cavity through the incision site. After flushing the peritoneal cavity, PMs were collected and centrifuged (1000 rpm for 2 min). To seed PMs, the cell density was adjusted to 3–5 $\times$ 10^6 cells/ml, and cells were incubated in Dulbecco's modified Eagle's medium. Total RNA was purified from the isolated SCN and PMs using TRIzol reagent (Invitrogen), and then 1 μg of total RNA was converted to complementary DNA (10 ng/ml) by room temperature. The resulting complementary DNA was used as a template for quantitative real-time PCR with the KAPA SYBR FAST qPCR kit (KAPA Biosystems, Boston, MA) using the ECOTM Real-Time PCR System (ASONE, Osaka, Japan). For semiquantitative PCR, GoTaq DNA polymerase (Promega) and a mixture of deoxynucleoside 5′-triphosphates (Promega) were used. PCR products were visualized by ethidium bromide staining after electrophoresis on a 1.5% agarose gel. The fluorescence intensities of PCR products were analyzed using ImageJ software (National Institutes of Health, Bethesda, MD) and were normalized based on *Gapdh* expression levels. Data are presented as expression ratios compared with those of *Gapdh*. Primers were purchased from Operon Biotechnology (Tokyo, Japan) and Hokkaido System Science (Hokkaido, Japan), and these sequences are shown in Table 1.

Flow Cytometry—PMs and T cells were analyzed by flow cytometry. After intravenous injection of liposome-clodronate or Clophosome-A^{TM} according to administration schedule described under the "Drug Administration," PMs were isolated from PSL-operated mice on days 4 or 7 after PSL. To stain macrophages, a single-cell suspension (1 $\times$ 10^6 cells) was incubated with fluorescein isothiocyanate (FITC)-conjugated anti-CD11b Ab, FITC-conjugated anti-CD14 Ab or phycoerythrin-conjugated anti-F4/80 Ab (eBioscience, San Diego, CA) in reaction buffer (1% fetal bovine serum and 0.05% NaN_3 in DMEM) for 30 min at 4 °C. FTY720 or PBS (containing 20% dimethyl sulfoxide) was administered according to the administration schedule described under the "Drug Administration." For isolation of T cells, peripheral blood was collected from the ophthalmic venous plexus on day 7 after PSL. Then, T cells were separated from peripheral blood cells using Lympholyte®-mammal (CEDARLANE). To stain T cells, a single-cell suspension (1 $\times$ 10^6 cells) was incubated with FITC-conjugated anti-CD4 Ab and phycoerythrin-conjugated anti-CD25 Ab (eBioscience) in reaction buffer for 30 min at 4 °C. After staining, cells were washed and resuspended in PBS containing 1% fetal bovine serum and 0.05% NaN_3. Data were acquired using a FACS Aria flow cytometer and analyzed using BD FACS Diva software (all from BD Bioscience).

TABLE 1
Sequences of PCR primers
The following primers were used for PCR amplification: *Gapdh*, glyceraldehyde-3-phosphate dehydrogenase; *Gitr*, glucocorticoid-induced tumor necrosis factor receptor; *Gitrl*, glucocorticoid-induced tumor necrosis factor receptor ligand; *Il-1β*, interleukin-1β; *Tnfα*, tumor necrosis factor-α.

Gene		Sequence
Semi-quantitative PCR		
Cd11b	Forward	5′-GTGCTGAGACTGGAGGCAAC-3′
	Reverse	5′-TCCACGCAGTCCGGTAAAAT-3′
Cd14	Forward	5′-GTGCTTGGCTTGTTGCTGTT-3′
	Reverse	5′-CGTAAGCCGCTTTAAGGACA-3′
Cd25	Forward	5′-AACGGCACCATCCTAAACTG-3′
	Reverse	5′-CACTCTGTCCTTCCACGAAA-3′
Cd4	Forward	5′-GTGGGTGTTCAAAGTGACCT-3′
	Reverse	5′-CCTTCTCTGCCTTCCACATC-3′
Gapdh	Forward	5′-TCCATGACAACTTTGGCATTGTGG-3′
	Reverse	5′-GTTGCTGTTGAAGTCGCAGGAGAC-3′
Gitr	Forward	5′-ACGGAAGTGGCAACAACACT-3′
	Reverse	5′-ACACAGCATTGTGGGTCTTG-3′
Gitrl	Forward	5′-AAGTCCTCAAAGGGCAGAGA-3′
	Reverse	5′-TACTACGAAGGGGGCATTGT-3′
Quantitative PCR		
Cd14	Forward	5′-GTGCTTGGCTTGTTGCTGTT-3′
	Reverse	5′-ACCAATCTGGCTTCGGATCT-3′
Gapdh	Forward	5′-GGGTGTGAACCACGAGAAAT-3′
	Reverse	5′-ACTGTGGTCATGAGCCCTTC-3′
Il-1β	Forward	5′-GCTGCTTCCAAACCTTTGAC-3′
	Reverse	5′-AGCTTCTCCACAGCCACAAT-3′
Tnfα	Forward	5′-CCCCAAAGGGATGAGAAGTT-3′
	Reverse	5′-TGGGCTACAGGCTTGTCACT-3′

Statistical Analysis—Appropriately sized samples for each experiment were based on our previous report (7, 16). Statistical analyses were performed using GraphPad Prism 5.0 (GraphPad Software, Inc.). We used all data obtained from each experiment, and performed randomization methods in all experiments. Data are presented as mean ± S.E. in all graphs. Data for gene expression generated using RT-PCR (Figs. 1, 4 and 8) and behavioral data from day 7 after nerve injury (Fig. 9) were analyzed using one-way analysis of variance, followed by post hoc Tukey's test. Time course data for behavioral experiments (Figs. 3, 5, 7, and 9) were analyzed using two-way analysis of variance with repeated measurements to detect interactions between drug treatments and different time points. After confirming statistical significance, Bonferroni multiple comparison tests were performed for intergroup comparisons and time point comparisons. The results of cell measurements (Figs. 1 and 10) were analyzed using an unpaired Student's *t* test (two-tailed). A threshold for statistical significance was set at $p < 0.05$.

RESULTS

Bone Marrow-derived Macrophages and T-cells Infiltrate the SCN after PSL—Initially, we evaluated the abundance of macrophages and T cells in the injured SCN after PSL (Fig. 1). We confirmed that PSL induced increased levels of macrophage-specific messenger RNA (mRNA) transcripts (*Cd11b* and *Cd14*) from days 3 to 7 after PSL (Fig. 1*A*), and T cell-specific mRNA transcripts (*Cd4* and *Cd25*) on day 7 after PSL in the injured SCN (Fig. 1*B*). Immunohistochemistry analysis showed the infiltration of F4/80$^+$ macrophages and CD4$^+$ T cells at the injured site of the SCN on day 7 after PSL, as compared with the sham-operated SCN (Fig. 1, *C* and *D*). To investigate whether these represented infiltrating (from the peripheral blood) or resident F4/80$^+$ macrophages and CD4$^+$ T cells, we performed

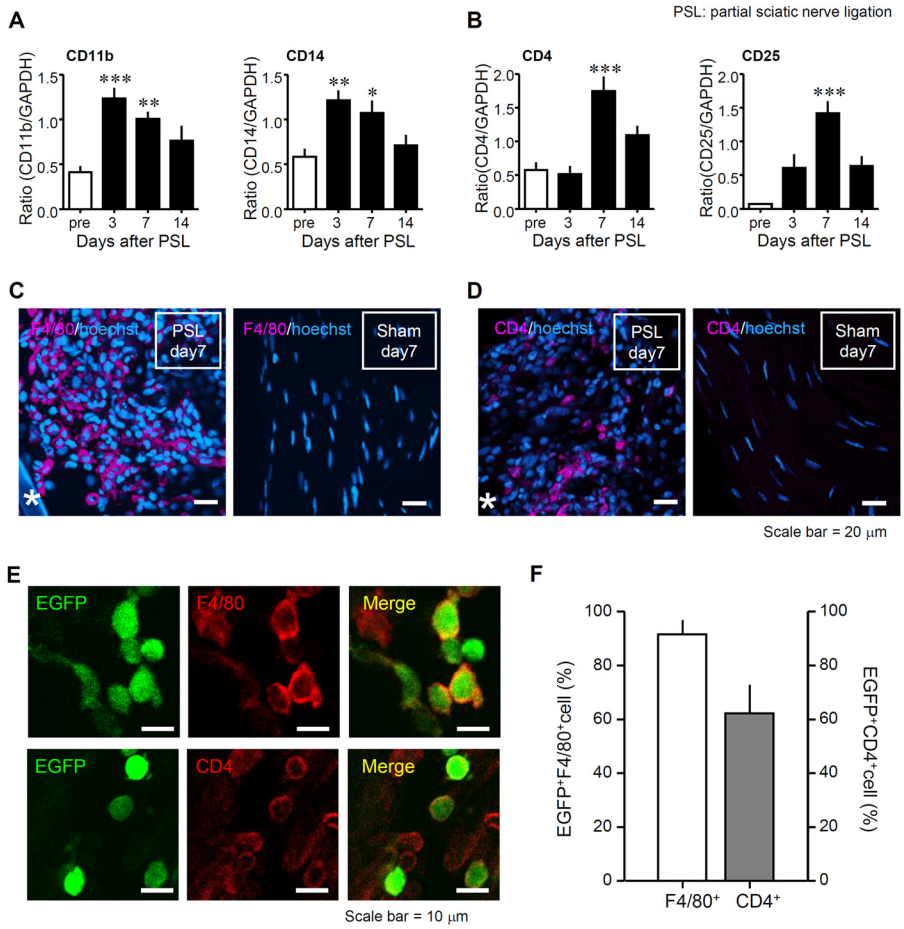

FIGURE 1. **Infiltration of bone marrow-derived macrophages and T cells at the injured SCN after PSL.** Mice underwent PSL or a sham operation, and then the SCN was collected. *A,* a time course of macrophage (*Cd11b* and *Cd14*) expression in the SCN on days 3, 7, and 14 after PSL. Gene expression levels were measured by RT-PCR, normalized to glyceraldehyde-3-phosphate dehydrogenase (*Gapdh*) and analyzed using ImageJ software (National Institutes of Health, Bethesda, MD). Data indicate mean ± S.E. for groups of 6 mice. *B,* a time course of T cell (*Cd4* and *Cd25*) marker in the SCN on days 3, 7, and 14 after PSL. Data indicate mean ± S.E. for groups of 12 mice; ***, $p < 0.001$; **, $p < 0.01$; and *, $p < 0.05$ compared with levels before PSL (*pre*). *C,* expression levels of F4/80 (macrophage marker) proteins in the SCN. *D,* expression levels of CD4 (a T cell marker) protein in the SCN. Representative micrographs on day 7 after PSL or sham operation were visualized by immunohistochemistry. *Magenta*, immune cell markers (F4/80 or CD4); *blue*, Hoechst 33342. *Asterisks* in micrographs indicate a silk suture used for SCN ligation. *Scale bars* = 20 μm. *E,* eGFP-chimeric mice after BMT received PSL, and the SCN was collected on day 7 after PSL. Co-localization of $eGFP^+$ cells and the macrophage (F4/80) or T cells (CD4) marker in the injured SCN after PSL. Representative micrographs on day 7 after PSL were visualized by immunohistochemistry. *Green*, eGFP; *red*, F4/80 or CD4; *yellow*, co-localized expression. *Scale bar* = 10 μm. *F,* the percentage of $eGFP^+F4/80^+$ cells (*white column*) and $eGFP^+CD4^+$ cells (*black column*) in the injured SCN on day 7 after PSL. The number of $F4/80^+$ cells or $eGFP^+F480^+$ cells was counted in each section (90,000 μm^2). The numbers of $CD4^+$ or $eGFP^+CD4^+$ cells were counted similarly. Both columns represent mean ± S.E. of groups of 5 SCN samples.

immunohistochemistry using eGFP-chimeric mice and evaluated the co-localization of eGFP and immune cell markers (macrophages, F4/80; T cells, CD4; Fig. 1*E*). The accumulation of $eGFP^+F4/80^+$ cells accounted for 92% of total $F4/80^+$ macrophages, and $eGFP^+CD4^+$ cells partially for 62% of total $CD4^+$ T cells (Fig. 1*F*). These results suggested that the macrophages and T cells that accumulated are at least partially derived from bone marrow, and migrated to the site injury in the SCN through peripheral circulation.

Macrophage Depletion Alleviates PSL-induced Neuropathic Pain—To assess the role of macrophages in neuropathic pain, we evaluated the effects of macrophage depletion agents, liposome-clodronate, and Clophosome-A™, on PSL-induced thermal hyperalgesia and tactile allodynia. Liposome-clodronate and Clophosome-A™ are known to deplete macrophages by inducing macrophage apoptosis (22). We confirmed the depletion of PMs after treatment with liposome-clodronate (Fig. 2, *A* and *C*) or Clophosome-A™ (Fig. 2, *B* and *D*) using flow cytometry. In the ipsilateral hind paw after PSL, a significant reduction in withdrawal latency to thermal stimuli and a significant increase in the number of withdrawal responses to a filament (0.07 g) were observed compared with the contralateral side, indicating thermal hyperalgesia and tactile allodynia, respectively. PSL-induced thermal hyperalgesia and tactile allodynia were suppressed in liposome-clodronate-treated mice on day 7 after PSL (Fig. 3*A*, *closed circle versus gray diamond*). Similarly, PSL-induced thermal hyperalgesia was suppressed by Clophosome-A™ on day 4 after PSL (Fig. 3*B*, *closed circle versus gray triangle*).

Inflammatory Cytokines Derived from Accumulated Macrophages in the Injured SCN Contribute to Neuroinflammation—To investigate the role of migrating macrophages in peripheral neuroinflammation, we assessed the effects of perineural injection of Clophosome-A™ on inflammatory cytokines that are normally up-regulated in the injured SCN after PSL. The mRNA up-regulation of *Cd14* (a macrophage marker) in the

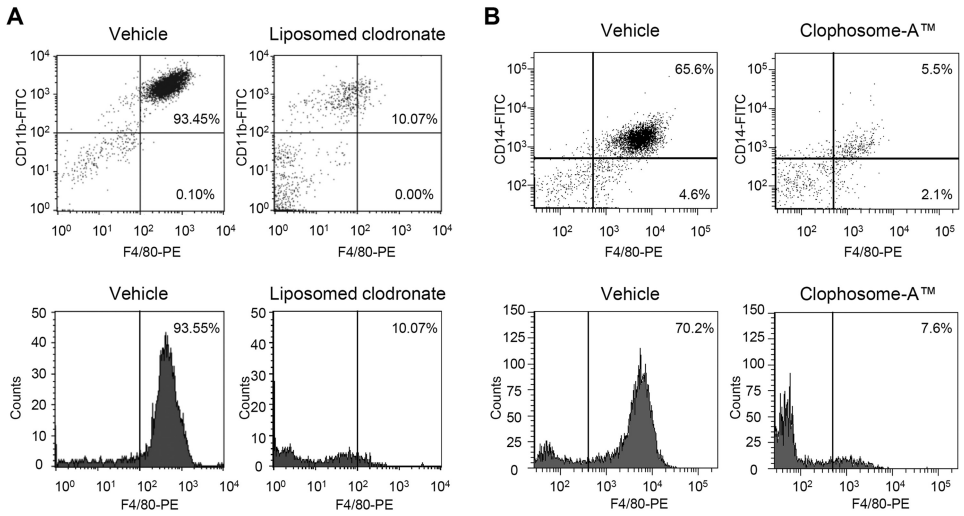

FIGURE 2. **Depletion of macrophages after clodronate treatment.** *A,* liposome-clodronate (1 mg in 0.2 ml, intravenously) or vehicle (phosphate-buffered saline) was administered twice to mice (1 day prior to PSL and 4 days after PSL), and PMs were collected on day 7 after PSL. The PM population was evaluated by flow cytometry using fluorescent monoclonal antibodies (*Abs*) for macrophages (FITC-conjugated anti-CD11b Ab and phycoerythrin (*PE*)-conjugated anti-F4/80 Ab). *B,* Clophosome-A™ (0.1 ml, i.v.; FormuMax Scientific, Palo Alto, CA) or vehicle (PBS) were administered once (1 day before PSL) to mice, and PMs were collected on day 4 after PSL. The PM population was quantified using FITC-conjugated anti-CD14 Ab and PE-conjugated anti-F4/80 Ab. *C* and *D,* histogram analysis shows the F4/80$^+$ macrophage counts after administration of liposome-clodronate or Clophosome-A™.

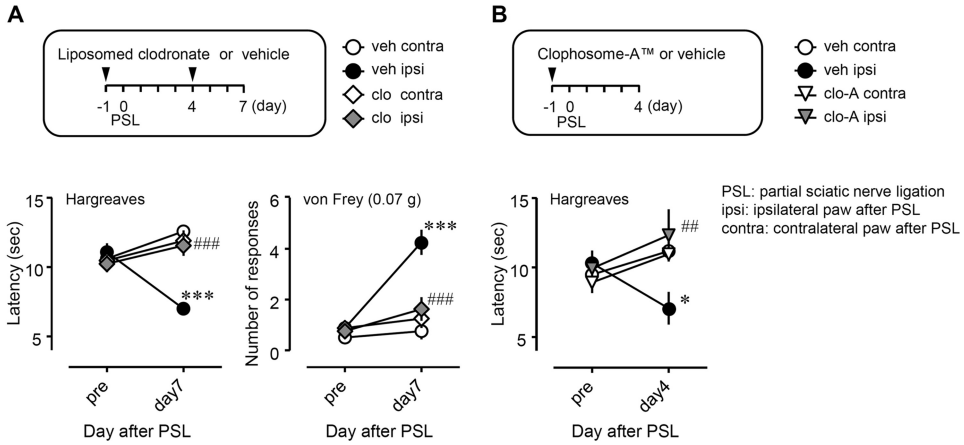

FIGURE 3. **Suppressive effects of systemic clodronate administration on PSL-induced thermal hyperalgesia and tactile allodynia.** Liposome-clodronate (*A,* 1 mg in 0.2 ml, i.v.) or Clophosome-A™ (*B,* 0.1 ml, i.v., FormuMax Scientific, Palo Alto, CA, USA) was injected as described under "Drug Administration." Thermal hyperalgesia and tactile allodynia were assessed by the Hargreaves test or the von Frey test, respectively. *clo*, liposome-clodronate; *clo-A*, Clophosome-A™; *veh*, vehicle (phosphate-buffered saline, PBS); *ipsi*, ipsilateral hind paw of the PSL-operated side; *contra*, contralateral hind paw of the PSL-operated side. Data indicate mean ± S.E. of groups of 8 (*A*) or 4 (*B*) mice; ***, $p < 0.001$ and *, $p < 0.05$ *versus* veh/contra; ###, $p < 0.001$, and ##, $p < 0.01$ *versus* veh/ipsi.

SCN on day 7 after PSL was significantly suppressed by Clophosome-A™. The up-regulation of *Il1β* and *Tnfα* mRNA was also abrogated in Clophosome-A™-treated mice (Fig. 4). Furthermore, we assessed the effect of perineural injection of Clophosome-A™ on the accumulation of T cells at the injured site of the SCN. By immunohistochemistry, PSL-induced accumulation of GITR$^+$ T cells was prevented by the perineural injection of Clophosome-A™ (Fig. 4*B*). The number of GITR$^+$ T cells in an area of 160,000 μm^2 was also reduced in Clophosome-A™-treated mice (Fig. 4*C*).

Peripheral Macrophages Maintain Neuropathic Pain after PSL—To elucidate the involvement of peripheral macrophages in the maintenance of neuropathic pain, we assessed pain responses after local injection of Clophosome-A™ to the injured SCN from day 7 after PSL (Fig. 5). Thermal hyperalgesia and tactile allodynia were established on day 7 after PSL, and continued until at least day 14. PSL-established thermal hyperalgesia and tactile allodynia were attenuated by perineural post-treatment with Clophosome-A™ (*closed circle versus gray triangle*).

Modulation of T Cell Function Alleviates PSL-induced Neuropathic Pain—Next, we examined the involvement of T cells in neuropathic pain. We confirmed the reduction of CD4$^+$ T cells in peripheral blood after treatment with FTY720, an immune modulator (Fig. 6). Surprisingly, the basal number of CD4$^+$CD25$^+$ T cells was low (less than 3% of total leukocytes) in the peripheral blood (Fig. 6*A*).

We assessed the effects of T cell depletion on neuropathic pain (Fig. 7). Thermal hyperalgesia and tactile allodynia on day 7 after PSL were attenuated by the repeated administration of FTY720 (Fig. 7*A*). Similarly, neutralizing anti-CD4 antibody had suppressive effects on both thermal hyperalgesia and tactile allodynia after PSL (Fig. 7*B*). However, these agents had no effect on pain thresholds on the contralateral side.

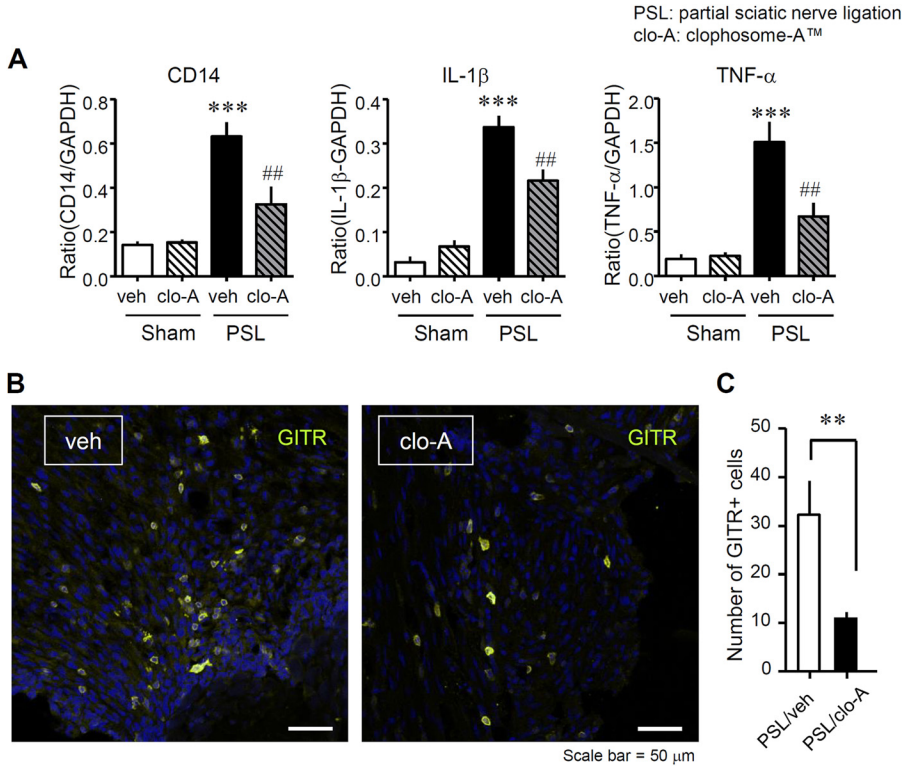

FIGURE 4. **Reduced expression of macrophages markers and inflammatory cytokines in the injured SCN after PSL in mice that received local administration of clodronate.** Clophosome-A™ (FormuMax Scientific, Palo Alto, CA) or vehicle (control liposomes for Clophosome-A™) was injected (10 μl) around the SCN every other day after PSL (*i.e.* on days 0, 2, 4, and 6 after PSL), and the SCN was collected on day 7 after PSL. *A*, the mRNA expression levels of *Cd14* (a macrophage marker), *interleukin-1β* (*Il1β*), and *tumor necrosis factor α* (*Tnfα*) levels after PSL were evaluated by quantitative reverse transcription-polymerase chain reaction. Gene expression levels were normalized to those of *glyceraldehyde-3-phosphate dehydrogenase* (*Gapdh*). Each column shows the mean intensity ratio compared with *Gapdh*. *clo-A*, Clophosome-A™; *veh*, vehicle (control liposomes). Data indicate mean ± S.E. of groups of 5 mice; ***, $p < 0.001$ *versus* Sham/veh; ###, $p < 0.001$, and ##, $p < 0.01$ *versus* PSL/veh. *B*, the presence of GITR$^+$ cells in vehicle-treated SCN or Clophosome-A™-treated SCN after PSL. Representative micrographs of slides stained using immunohistochemistry show the SCN on day 7 after PSL. *Yellow*, GITR; *blue*, Hoechst 33342. *Scale bar* = 50 μm. *C*, the number of GITR$^+$ cells in the SCN after Clophosome-A™ treatment. Total GITR$^+$ cells were counted in each section (160,000 μm^2). Both columns represent mean ± S.E. of groups of 11 SCN samples; **, $p < 0.01$ *versus* PSL/veh. *clo-A*, Clophosome-A™; *veh*, vehicle (control liposomes).

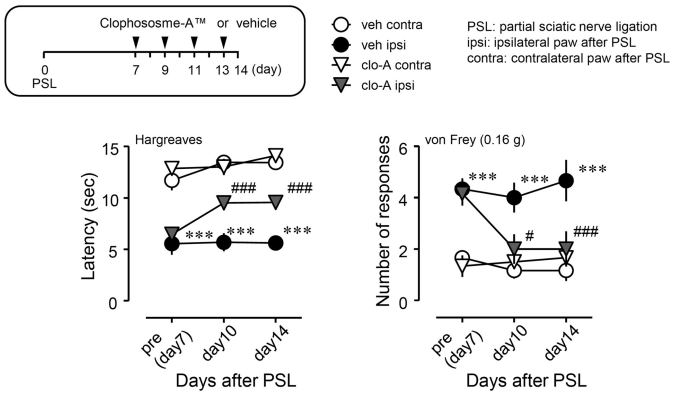

FIGURE 5. **Inhibitory effects of the local administration of clodronate on PSL-induced thermal hyperalgesia and tactile allodynia.** Clophosome-A™ (FormuMax Scientific) or vehicle (control liposomes) was injected (10 μl) around the sciatic nerve every other day after PSL, and the injection started on day 7 after PSL (*i.e.* on days 7 (*pre*), 9, 11, and 13 after PSL). Thermal hyperalgesia and tactile allodynia were assessed by the Hargreaves test or the von Frey test, respectively. *clo-A*, Clophosome-A™; *veh*, vehicle (control liposomes); *ipsi*, ipsilateral hind paw of the PSL-operated side; *contra*, contralateral hind paw of the PSL-operated side. Data shown indicate mean ± S.E. of groups of 6 mice; ***, $p < 0.001$ *versus* veh/contra; ###, $p < 0.001$ and #, $p < 0.05$ *versus* veh/ipsi.

PSL Induces the Up-regulation of GITRL and GITR in the Injured SCN—We measured mRNA expression levels of *Gitrl* and *Gitr* in the injured SCN after PSL by RT-PCR (Fig. 8). The mRNA expression levels of *Gitrl* and *Gitr* were increased in the injured SCN after PSL (Fig. 8, *A* and *B*). Generally, GITRL is expressed by antigen presenting cells, including macrophages, whereas GITR is most abundantly expressed by activated T cells. These observations were consistent with our findings that the mRNA expression levels of *Gitrl*, but not *Gitr*, were elevated in PMs (Fig. 8*B*).

To characterize the localization of GITRL and GITR in the injured SCN after PSL, we performed double-immunostaining using immune cell markers. The number of GITRL$^+$ cells increased in the injured SCN after PSL, and GITRL expression was confined to F4/80$^+$ macrophages (Fig. 8*C*). Moreover, the number of GITR$^+$ cells was also increased, and partially co-localized with CD4$^+$ T cells (Fig. 8*D*).

Inhibiting the GITRL-GITR Pathway by Neutralizing GITRL Antibody Suppresses PSL-induced Neuropathic Pain—To evaluate the function of the GITRL-GITR pathway in the injured SCN after PSL, we characterized the effects of anti-GITRL antibody on PSL-induced thermal hyperalgesia and tactile allodynia (Fig. 9). On the ipsilateral side, thermal hyperalgesia after PSL was prominently suppressed by the perineural injection of anti-GITRL antibody (Fig. 9*A*, *closed circle versus gray diamond*). The number of withdrawal responses increased after PSL, and also were attenuated by anti-GITRL antibody (Fig. 9*B*). Anti-GITRL antibody had no effect on thermal hyperalge-

sia and tactile allodynia on the contralateral side (Fig. 9, *A* and *B, open circle versus open diamond*). On day 7 after PSL, the perineural injection of anti-GITRL antibody attenuated PSL-induced thermal hyperalgesia and tactile allodynia in a dose-dependent manner (Fig. 9, *C* and *D*). Similar to our above findings for the number of withdrawal responses, anti-GITRL antibody increased the 50% withdrawal threshold, which decreased following PSL (Fig. 9*E*). These data suggested that inhibition of the GITRL-GITR pathway could suppress PSL-induced thermal hyperalgesia and tactile allodynia.

Perineural Injection of Neutralizing GITRL Antibody Prevented the Migration of Macrophages and T Cells into the Injured SCN after PSL—To evaluate the effects of anti-GITRL antibody on the infiltration of macrophages and T cells to injured site of the SCN on day 7 after PSL, we counted the number of F4/80$^+$ macrophages and CD4$^+$ T cells after the perineural injection of anti-GITRL antibody. After treatment with anti-GITRL antibody, the number of both macrophages (Fig. 10*A*) and T cells (Fig. 10*B*) were decreased as compared with the control IgG treatment.

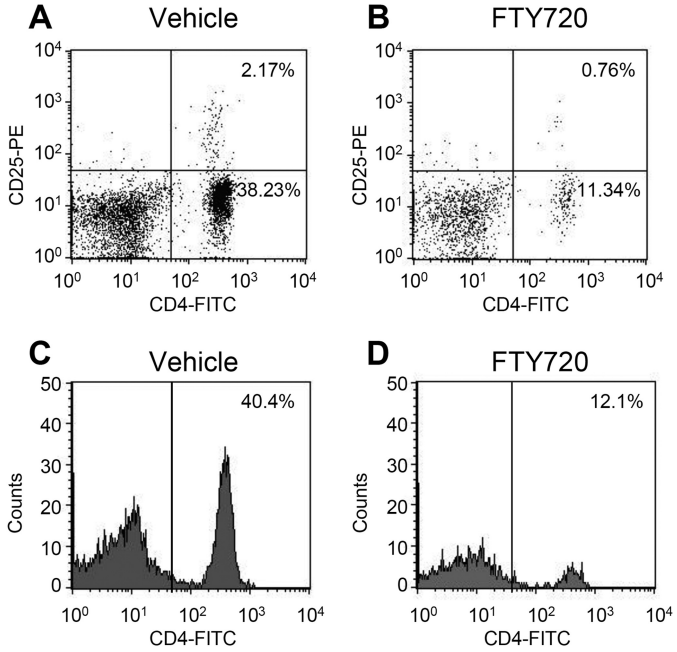

FIGURE 6. **Reduction in CD4$^+$ T cell numbers after treatment with FTY720.** FTY720 (0.1 mg/kg) or vehicle (phosphate-buffered saline containing 20% dimethyl sulfoxide) was injected intraperitoneally daily for 8 days (days 0–7) after PSL, and peripheral blood was collected on day 7 after PSL. T cell populations in the peripheral blood were evaluated by flow cytometry using fluorescent antibodies for T cells (FITC-conjugated anti-CD4 Ab and phycoerythrin (*PE*)-conjugated anti-CD25 Ab). *A* and *B,* dot plot analyses show CD4$^+$ and CD25$^+$ T cell populations. *C* and *D,* histogram analyses shows CD4$^+$ T cell counts.

DISCUSSION

We demonstrated that the accumulation of macrophages and T cells around the injured SCN contributes to PSL-induced neuropathic pain through the GITRL system. Macrophages might activate T cells and facilitate neuroinflammation, resulting in neuropathic pain. Although there are several lines of evidence that support an important role for immune cells (3–5), the pathophysiological role of cell-cell interactions in neuropathic pain is poorly understood. Thus, this report is the first to reveal an essential role for macrophage-driven T cell activation through the GITRL-GITR pathway in neuropathic pain.

After peripheral nerve injury, activation of immune cells can trigger neuroinflammation via cytokine-chemokine networks, resulting in the development of neuropathic pain (23–25). Because nerve injury can result in the breakdown of the blood-nerve barrier in the peripheral nervous systems, peripheral leukocytes can then extravagate and drive neuroinflammation, resulting in neuropathic pain (4, 5).

In this study, we found that many macrophages infiltrated into the injured SCN after PSL. We also observed that BM-derived eGFP$^+$F4/80$^+$ cells migrated around the injured nerve, indicating that infiltrating macrophages in the injured site of the SCN were derived from circulating monocytes. Deple-

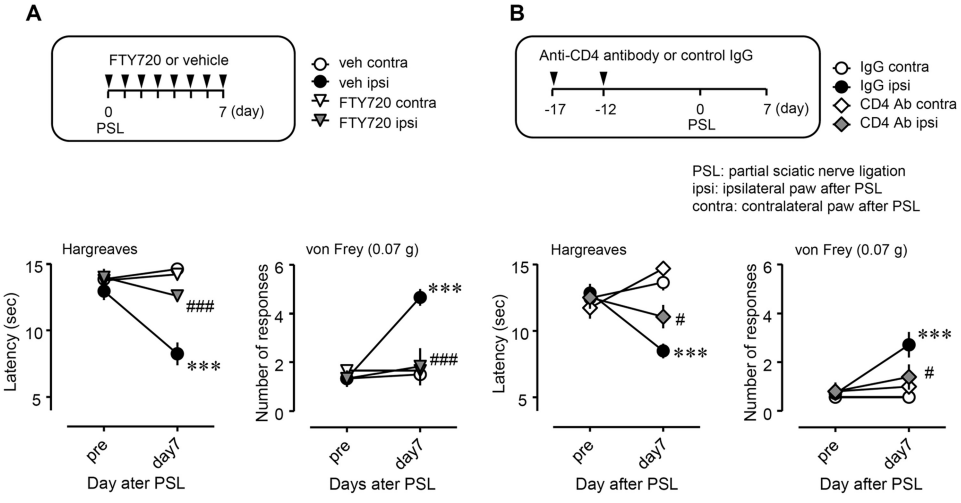

FIGURE 7. **Suppressive effects of FTY720 and anti-CD4 antibody on PSL-induced thermal hyperalgesia and tactile allodynia.** *A,* FTY720 (0.1 mg/kg, $n = 6$) or vehicle (phosphate-buffered saline containing 20% dimethyl sulfoxide, $n = 6$) was injected intraperitoneally. *B,* anti-CD4 antibody (CD4 Ab; diluted 1:5) with phosphate-buffered saline ($n = 5$) or control immune globulin G (IgG, $n = 7$) was injected (0.2 ml) via the tail vein. Thermal hyperalgesia and tactile allodynia were assessed by the Hargreaves test or von Frey test, respectively, on day 7 after PSL. *veh*, vehicle; *IgG*, control IgG; *ipsi*, ipsilateral hind paw of the PSL-operated side; contra, contralateral hind paw of the PSL-operated side. Data shown indicate mean ± S.E.; ***, $p < 0.001$ *versus* veh contra or IgG contra; ###, $p < 0.001$, and #, $p < 0.05$ *versus* vehicle ipsi or IgG ipsi.

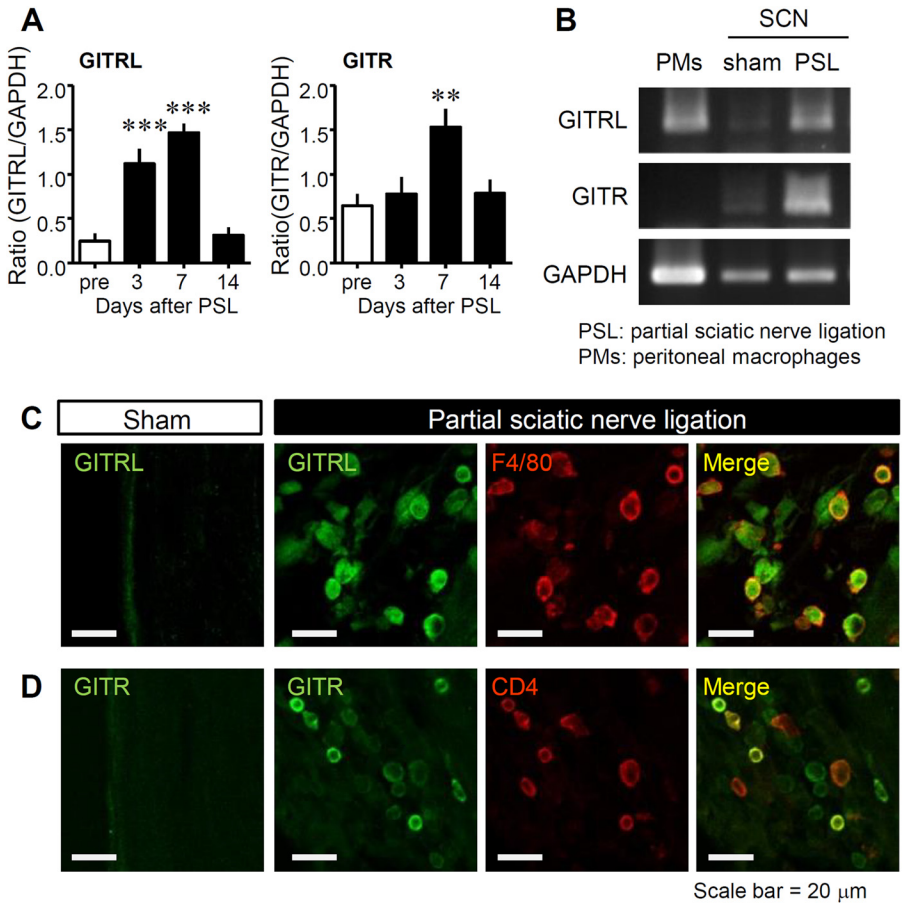

FIGURE 8. **Expression of GITRL and GITR in the SCN after PSL and murine PMs.** *A,* the time course of GITRL (*Gitrl*) and GITR (*Gitr*) induction in the SCN on days 3, 7, and 14 after PSL. Gene expression levels measured by reverse transcription polymerase chain reaction were normalized to levels of glyceraldehyde-3-phosphate dehydrogenase (*Gapdh*) expression and analyzed using ImageJ software (National Institutes of Health). Data indicate mean ± S.E. for groups of 12 mice; ***, $p < 0.001$, and **, $p < 0.01$, compared with levels before PSL. *B,* the gene expression levels of *Gitrl*, *Gitr*, and *Gapdh* in naive murine PMs and in the SCN after PSL or sham operation on day 7. *C* and *D,* localization of GITRL and GITR in the injured SCN. Representative micrographs of sections stained using immunohistochemistry show the SCN on day 7 after PSL or sham operation. Co-localization of GITRL and macrophage (F4/80) or T cell (CD4) markers is shown. *Green*, GITRL or GITR; *red*, F4/80 or CD4; *yellow*, co-localized expression. *Scale bar* = 20 μm.

tion of systemic macrophages suppressed PSL-induced thermal hyperalgesia and tactile allodynia after PSL. These findings suggested that macrophages recruited from peripheral blood vessels might be an important factor in neuropathic pain. Next, to examine the role of infiltrating macrophages around the injured SCN, we locally administered Clophosome-A™ into the injured SCN. Macrophage depletion by the perineural injection of Clophosome-A™ suppressed the up-regulation of IL-1β and TNF-α, as well as reduced the number of $GITR^+$ T cells in the injured SCN after PSL. Currently available evidence supports the concept that macrophage-derived chemoattracting soluble factors, such as IL-1β and TNF-α, induce the migration of T cells and elicit neuroinflammation. The local depletion of macrophages by Clophosome-A™ also attenuated PSL-induced thermal hyperalgesia and tactile allodynia, even when administered post-treatment from day 7 after PSL. Other studies have shown that the accumulation of macrophages in the injured SCN can persist for more than 1 month after nerve injury (26). Thus, macrophages, which are critical cells for peripheral neuroinflammation, play a crucial role in both the development and maintenance of neuropathic pain.

We also showed the contribution of T cells, which control the immune response, to neuropathic pain. Our data indicated that the mRNA expression levels of T cell markers (*Cd4* and *Cd25*) were increased by PSL, and persisted until at least day 14 after PSL. $CD4^+$ T cells also infiltrated the injured site of the SCN on day 7 after PSL. Although all of these $CD4^+$ T cells were not derived from the bone marrow, at least some of the $CD4^+$ cells had migrated from peripheral blood vessels.

Sequestration of T cells in lymphoid organs by administering FTY720 or depleting $CD4^+$ T cells by treatment with anti-CD4 antibody attenuated thermal hyperalgesia and tactile allodynia after PSL. Recent reports have shown that FTY720 could suppress formalin-induced inflammatory pain and spare nerve injury-induced neuropathic pain (17), indicating an important role for $CD4^+$ T cells in neuroinflammation. FTY720 reduces the number of T cells in the peripheral blood by preventing the egress of T cells from the thymus and lymph nodes, leading to a marked reduction of T cells in circulation (18). T cells exhibit diverse phenotypes after differentiation from naive T cells, such as proinflammatory T helper (Th) type 1 cells and anti-inflammatory Th2 cells. Importantly, Th17 cells are a newly described lineage of effector T cells that produce IL-17 and contribute to neuropathic pain (26, 27). By contrast, Treg are negative regulators of immune activation that act to prevent excessive autoimmunity and play a crucial role in the maintenance of immune

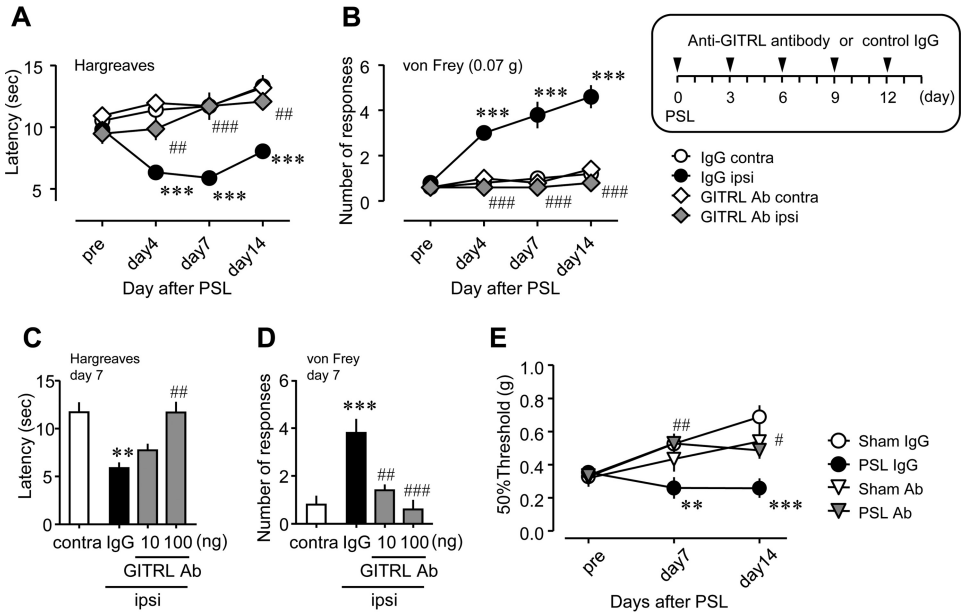

FIGURE 9. **Therapeutic effects of anti-GITRL antibody on PSL-induced thermal hyperalgesia and tactile allodynia.** Anti-GITRL antibody (*GITRL Ab*; 10 or 100 ng) or control immunoglobulin G (IgG) was perineurally administered (10 μl) five times (on days 0, 3, 6, 9, and 12 after PSL). Thermal hyperalgesia and tactile allodynia were assessed by the Hargreaves test or the von Frey test, respectively. *A* and *B,* a time course of the suppressive effect of GITRL Ab on PSL-induced thermal hyperalgesia and tactile allodynia. *C* and *D,* dose-dependent effects of GITRL Ab on PSL-induced thermal hyperalgesia and tactile allodynia. *IgG*, control IgG; *ipsi*, ipsilateral hind paw of the PSL-operated side; *contra*, contralateral hind paw of the PSL-operated side. Data shown indicate mean ± S.E. of groups of five mice; ***, $p < 0.001$ and **, $p < 0.01$ *versus* IgG contra; ###, $p < 0.001$, and ##, $p < 0.01$ *versus* IgG ipsi. *E*, effects of GITRL Ab on the 50% withdrawal threshold after PSL. GITRL Ab was perineurally injected according to the administration schedule. Data shown indicate mean ± S.E. of groups of 5–8 mice; ***, $p < 0.001$ and **, $p < 0.01$ *versus* sham IgG; ##, $p < 0.01$, and #, $p < 0.05$ *versus* PSL IgG.

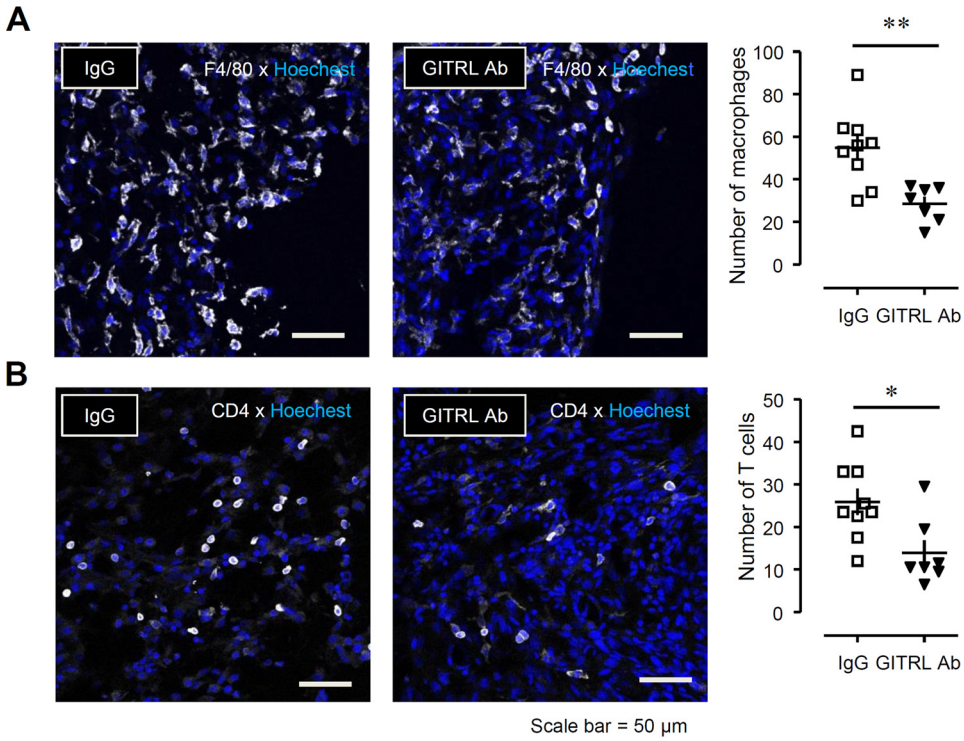

FIGURE 10. **Suppressive effects of neutralizing anti-GITRL antibody on the migration of F4/80$^+$ macrophages and CD4$^+$ T cells into the injured SCN after PSL.** Anti-GITRL antibody (*GITRL Ab*; 100 ng) or control immunoglobulin G (IgG) was perineurally administered (10 μl) three times (on days 0, 3, and 6 after PSL) to mice. The SCN was collected on day 7 after PSL. *A,* the number of F4/80$^+$ cells in the SCN after treatment with IgG or GITRL Ab. *B,* the number of CD4$^+$ cells in the SCN after treatment with IgG or GITRL Ab. Total F4/80$^+$ or CD4$^+$ cells were counted in each section (90,000 μm^2). *White*, F4/80 or CD4; *blue*, Hoechst. *Scale bar* = 50 μm. Each value indicates the measured value and mean ± S.E. of groups of 7–9 SCN samples; **, $p < 0.01$ and *, $p < 0.05$ *versus* IgG.

homeostasis (28). We found that circulating CD4$^+$CD25$^+$ T cells in vehicle-treated PSL mice were present at a low level (2.17%), whereas CD4$^+$ T cells represented 40.4% of peripheral leukocytes. Because CD25, a common marker of activated T cells (29), is also expressed by naturally occurring Treg cells (30), we postulated that the increased levels of Cd25 mRNA

indicated the accumulation of Treg cells in the injured SCN. However, because $CD4^+CD25^+$ Treg cells are quite low in the peripheral blood after nerve injury, it is possible that $CD4^+CD25^+$ Treg cells function poorly in this pain model. Another report has shown that enhancing the proliferation of Treg cells in the injured SCN can reduce chronic constriction injury-induced neuropathic pain (31). Thus, we speculate that the balance between proinflammatory $CD4^+$ Th1 and Th17 cells and anti-inflammatory $CD4^+CD25^+$ Treg cells is very important in the regulation of neuropathic pain. Further studies will be needed to elucidate the function of Treg cells in neuropathic pain.

We further focused on membrane-associated proteins that act as co-stimulatory molecules to regulate immune responses. By RT-PCR and immunohistochemistry, we considered that the up-regulation of GITRL and GITR after PSL was a consequence of the accumulation of macrophages and T cells in the injured SCN after PSL. Because the frequency of $CD4^+CD25^+$ Treg cells in the peripheral blood was very low, we predict that GITR-expressing cells might be $CD4^+$ effector T cells (Th1 and Th17 cells).

In our behavioral analyses, inhibition of the GITRL-GITR pathway by anti-GITRL antibody significantly attenuated PSL-induced thermal hyperalgesia and tactile allodynia, indicating that the GITRL-GITR pathway acts on macrophages and T cells in the injured SCN and promotes neuropathic pain. Anti-GITRL antibody also suppressed the migration of $F4/80^+$ macrophages and $CD4^+$ T cells to the injured site of the SCN. However, GITRL is not a chemoattractant. GITRL is a membrane-associated protein expressed by macrophages, and is not released from macrophages. Thus, we predicted that inactivation of macrophages was induced by anti-GITRL antibody, resulting in the suppression of autocrine chemoattractant, such as IL-1β and TNF-α, production by macrophages. Consequently, the migration of $CD4^+$ T cells was prevented.

To date, it has been reported that the GITRL-GITR pathway could be a novel therapeutic target in several diseases. Mice lacking the *Gitrl* gene show attenuated spinal inflammation after spinal cord injury and intestinal inflammation (32, 33). Moreover, inhibition of the GITRL-GITR pathway by anti-GITRL antibody prevented the development of autoimmune diabetes (14). These findings support our present study that shows the key role of cell-cell interactions between macrophages and T cells via the GITRL-GITR pathway in PSL-induced neuroinflammation.

In conclusion, we propose that macrophages drive T cell activation through the GITRL-GITR pathway, which plays a critical role in PSL-induced neuropathic pain. Inhibition of the GITRL-GITR pathway might represent a potential strategy for treating neuropathic pain.

Acknowledgments—We thank Akio Tamano and Aya Sakaguchi (both undergraduate students from Wakayama Medical University, Wakayama, Japan) for providing technical assistance.

REFERENCES

1. Baron, R. (2006) Mechanisms of disease: neuropathic pain, a clinical perspective. *Nat. Clin. Pract. Neurol.* **2,** 95–106
2. Campbell, J. N., and Meyer, R. A. (2006) Mechanisms of neuropathic pain. *Neuron* **52,** 77–92
3. Marchand, F., Perretti, M., and McMahon, S. B. (2005) Role of the immune system in chronic pain. *Nat. Rev. Neurosci.* **6,** 521–532
4. Calvo, M., Dawes, J. M., and Bennett, D. L. (2012) The role of the immune system in the generation of neuropathic pain. *Lancet Neurol.* **11,** 629–642
5. Scholz, J., and Woolf, C. J. (2007) The neuropathic pain triad: neurons, immune cells and glia. *Nat. Neurosci.* **10,** 1361–1368
6. Thacker, M. A., Clark, A. K., Marchand, F., and McMahon, S. B. (2007) Pathophysiology of peripheral neuropathic pain: immune cells and molecules. *Anesth. Analg.* **105,** 838–847
7. Kiguchi, N., Maeda, T., Kobayashi, Y., Fukazawa, Y., and Kishioka, S. (2010) Macrophage inflammatory protein-1α mediates the development of neuropathic pain following peripheral nerve injury through interleukin-1β up-regulation. *Pain* **149,** 305–315
8. Kiguchi, N., Kobayashi, Y., Maeda, T., Fukazawa, Y., Tohya, K., Kimura, M., and Kishioka, S. (2012) Epigenetic augmentation of the macrophage inflammatory protein 2/C-X-C chemokine receptor type 2 axis through histone H3 acetylation in injured peripheral nerves elicits neuropathic pain. *J. Pharmacol. Exp. Ther.* **340,** 577–587
9. Saika, F., Kiguchi, N., Kobayashi, Y., Fukazawa, Y., and Kishioka, S. (2012) CC-chemokine ligand 4/macrophage inflammatory protein-1β participates in the induction of neuropathic pain after peripheral nerve injury. *Eur. J. Pain* **16,** 1271–1280
10. Nocentini, G., Giunchi, L., Ronchetti, S., Krausz, L. T., Bartoli, A., Moraca, R., Migliorati, G., and Riccardi, C. (1997) A new member of the tumor necrosis factor/nerve growth factor receptor family inhibits T cell receptor-induced apoptosis. *Proc. Natl. Acad. Sci. U.S.A.* **94,** 6216–6221
11. Gurney, A. L., Marsters, S. A., Huang, R. M., Pitti, R. M., Mark, D. T., Baldwin, D. T., Gray, A. M., Dowd, A. D., Brush, A. D., Heldens, A. D., Schow, A. D., Goddard, A. D., Wood, W. I., Baker, K. P., Godowski, P. J., and Ashkenazi, A. (1999) Identification of a new member of the tumor necrosis factor family and its receptor, a human ortholog of mouse GITR. *Curr. Biol.* **9,** 215–218
12. Shevach, E. M., and Stephens, G. L. (2006) The GITR-GITRL interaction: co-stimulation or contrasuppression of regulatory activity? *Nat. Rev. Immunol.* **6,** 613–618
13. Cuzzocrea, S., Nocentini, G., Di Paola, R., Agostini, M., Mazzon, E., Ronchetti, S., Crisafulli, C., Esposito, E., Caputi, A. P., and Riccardi, C. (2006) Proinflammatory role of glucocorticoid-induced TNF receptor-related gene in acute lung inflammation. *J. Immunol.* **177,** 631–641
14. You, S., Poulton, L., Cobbold, S., Liu, C. P., Rosenzweig, M., Ringler, D., Lee, W. H., Segovia, B., Bach, J. F., Waldmann, H., and Chatenoud, L. (2009) Key role of the GITR/GITRLigand pathway in the development of murine autoimmune diabetes: a potential therapeutic target. *PLoS One* **4,** e7848
15. Seltzer, Z., Dubner, R., and Shir, Y. (1990) A novel behavioral model of neuropathic pain disorders produced in rats by partial sciatic nerve injury. *Pain* **43,** 205–218
16. Kobayashi,Y. K., Kiguchi, N., Maeda, T., Ozaki, M., and Kishioka, S. (2012) The critical role of spinal ceramide in the development of partial sciatic nerve ligation-induced neuropathic pain in mice. *Biochem. Biophys. Res. Commun.* **421,** 318–322
17. Coste, O., Pierre, S., Marian, C., Brenneis, C., Angioni, C., Schmidt, H., Popp, L., Geisslinger, G., and Scholich, K. (2008) Antinociceptive activity of the S1P-receptor agonist FTY720. *J. Cell Mol. Med.* **12,** 995–1004
18. Brinkmann, V., Davis, M. D., Heise, C. E., Albert, R., Cottens, S., Hof, R., Bruns, C., Prieschl, E., Baumruker, T., Hiestand, P., Foster, C. A., Zollinger, M., and Lynch, K. R. (2002) The immune modulator FTY720 targets sphingosine 1-phosphate receptors. *J. Biol. Chem.* **277,** 21453–21457
19. Okada, Y., Reinach, P. S., Shirai, K., Kitano, A., Kao, W. W., Flanders, K. C., Miyajima, M., Liu, H., Zhang, J., and Saika, S. (2011) TRPV1 involvement in inflammatory tissue fibrosis in mice. *Am. J. Pathol.* **178,** 2654–2664
20. Kiguchi, N., Kobayashi, Y., Maeda, T., Tominaga, S., Nakamura, J., Fukazawa, Y., Ozaki, M., and Kishioka, S. (2012) Activation of nicotinic acetylcholine receptors on bone marrow-derived cells relieves neuropathic pain accompanied by peripheral neuroinflammation. *Neurochem. Int.* **61,** 1212–1219

21. Hargreaves, K., Dubner, R., Brown, F., Flores, C., and Joris, J. (1988) A new and sensitive method for measuring thermal nociception in cutaneous hyperalgesia. *Pain* **32,** 77–88
22. Van Rooijen, N., and Sanders, A. (1994) Liposome mediated depletion of macrophages: mechanism of action, preparation of liposomes and applications. *J. Immunol. Methods* **174,** 83–93
23. Kiguchi, N., Kobayashi, Y., and Kishioka, S. (2012) Chemokines and cytokines in neuroinflammation leading to neuropathic pain. *Curr. Opin. Pharmacol.* **12,** 55–61
24. Wei, X. H., Zang, Y., Wu, C. Y., Xu, J. T., Xin, W. J., and Liu, X. G. (2007) Peri-sciatic administration of recombinant rat TNF-α induces mechanical allodynia via upregulation of TNF-α in dorsal root ganglia and in spinal dorsal horn: the role of NF-κB pathway. *Exp. Neurol.* **205,** 471–484
25. Zelenka, M., Schäfers, M., and Sommer, C. (2005) Intraneural injection of interleukin-1β and tumor necrosis factor-α into rat sciatic nerve at physiological doses induces signs of neuropathic pain. *Pain* **116,** 257–263
26. Li, J. J., Zhou, X., and Yu, L. C. (2005) Involvement of neuropeptide Y and Y1 receptor in antinociception in the arcuate nucleus of hypothalamus, an immunohistochemical and pharmacological study in intact rats and rats with inflammation. *Pain* **118,** 232–242
27. Kleinschnitz, C., Hofstetter, H. H., Meuth, S. G., Braeuninger, S., Sommer, C., and Stoll, G. (2006) T cell infiltration after chronic constriction injury of mouse sciatic nerve is associated with interleukin-17 expression. *Exp. Neurol.* **200,** 480–485
28. Steward-Tharp, S. M., Song, Y. J., Siegel, R. M., and O'Shea, J. J. (2010) New insights into T cell biology and T cell-directed therapy for autoimmunity, inflammation, and immunosuppression. *Ann. N.Y. Acad. Sci.* **1183,** 123–148
29. Taniguchi, T., and Minami, Y. (1993) The IL-2/IL-2 receptor system: a current overview. *Cell* **73,** 5–8
30. Hall, B. M., Verma, N. D., Tran, G. T., and Hodgkinson, S. J. (2011) Distinct regulatory $CD4^+$ T cell subsets: differences between naive and antigen specific T regulatory cells. *Curr. Opin. Immunol.* **23,** 641–647
31. Austin, P. J., Kim, C. F., Perera, C. J., and Moalem-Taylor, G. (2012) Regulatory T cells attenuate neuropathic pain following peripheral nerve injury and experimental autoimmune neuritis. *Pain* **153,** 1916–1931
32. Nocentini, G., Cuzzocrea, S., Genovese, T., Bianchini, R., Mazzon, E., Ronchetti, S., Esposito, E., Rosanna, D. P., Bramanti, P., and Riccardi, C. (2008) Glucocorticoid-induced tumor necrosis factor receptor-related (GITR)-Fc fusion protein inhibits GITR triggering and protects from the inflammatory response after spinal cord injury. *Mol. Pharmacol.* **73,** 1610–1621
33. Liao, G., van Driel, B., Magelky, E., O'Keeffe, M. S., de Waal Malefyt, R., Engel, P., Herzog, R. W., Mizoguchi, E., Bhan, A. K., and Terhorst, C. (2014) Glucocorticoid-induced TNF receptor family related protein ligand regulates the migration of monocytes to the inflamed intestine. *FASEB J.* **28,** 474–484